LA-UR-15-27858
Approved for public release; distribution is unlimited.

Title: MCNP6 GENXS Option Expansion to Include Fragment Spectra of Heavy Ions

Author(s): Kerby, Leslie Marie
Mashnik, Stepan Georgievich
Bull, Jeffrey S.

Intended for: PHYSOR 2016, 2016-05-01/2016-05-05 (Sun Valley, Idaho, United States)

Issued: 2016-02-22 (rev.1)

MCNP6 GENXS Option Expansion to Include Fragment Spectra of Heavy Ions

Leslie M. Kerby[1,2], **Stepan G. Mashnik**[2], **and Jeffrey S. Bull**[2]
[1] Nuclear Engineering and Health Physics
Idaho State University, Pocatello, Idaho, USA
[2] XCP-3: Monte Carlo Codes
Los Alamos National Laboratory, Los Alamos, New Mexico, USA
kerblesl@isu.edu

ABSTRACT

The GENXS option allows for various production cross sections to be tallied in MCNP6 for high-energy applications, including applications in space research, medical physics, and accelerators, among others. Previously, double differential cross sections (cross section per emitted fragment energy and angle) were only available for fragments up to ^{4}He. This expansion includes the ability to tally and output double differential cross sections for any heavy ion (with valid ZAID). It also includes the ability to tally and output angle-integrated cross sections per emitted fragment energy or energy-integrated cross sections per angle, for any ZAID.

Key Words: **MCNP6, GENXS, cross sections, high-energy**

1. INTRODUCTION

The Computational Physics group 3 (Monte Carlo Codes) within the X Division at Los Alamos National Laboratory (LANL) has led the development of the transport code MCNP6 (Monte Carlo N-Particle transport code, version 6) [1]. MCNP6 is a general-purpose, continuous-energy, generalized-geometry, time-dependent, Monte Carlo radiation-transport code designed to track many particle types over broad ranges of energies. It is used around the world in applications ranging from radiation protection and dosimetry, nuclear reactor design, nuclear criticality safety, detector design and analysis, decontamination and decommissioning, accelerator applications, medical physics, to space research and beyond. At higher energies (> 150 MeV) MCNP6 uses the Cascade Exciton Model version 03.03 (CEM03.03) [2, 3] and the Los Alamos Quark-Gluon String Model version 03.03 (LAQGSM03.03) [3, 4] to model nuclear reactions.

At these higher energies (> 150 MeV), the GENXS option can be used to tally fragment production cross sections. This is useful in an array of applications, including space research, medical physics, and accelerator applications, to name just a few. Previously, double differential cross sections (cross section per emitted fragment energy and angle) were only available for fragments up to ^{4}He. (See Ref. [5] for details on the original GENXS.) The upgrade discussed in this paper includes the ability to

tally and output double differential cross sections for any heavy ion (with valid ZAID). It also includes the ability to tally and output angle-integrated cross sections per emitted fragment energy or energy-integrated cross sections per angle, for any ZAID.

2. MCNP6 AND GENXS EXAMPLE INPUT FILES

A sample MCNP6 input using GENXS is displayed below:

```
MCNP6 test: Spectra from 200 MeV p + Al27 by CEM03.03
c Cells
1 1000 -2.7 -100 200 -300
2 0 -400(100:-200:300)
3 0 400

c ——————————————————————
c Surfaces
100 cz 4.0
200 pz -1.0
300 pz 1.0
400 so 50.0

c ——————————————————————
c Materials
m1000 13027 1.0
c
sdef erg=200 par=H dir=1 pos=0 0 0 vec 0 0 1
imp:h 1 1 0
phys:h 300
mode h n a #
LCA 8j 1 $ use CEM03.03
tropt genxs inxcp200al nreact on nescat off
c ——————————————————————
print 40 110 95
nps 10000000
prdmp 2j -1
```

This example simulates the nuclear spallation reaction of 200 MeV protons striking ^{27}Al. Note that in order to tally double differential cross sections of heavy ions, heavy ions (#) must be added to the MODE card. As explained in Ref. [5], the GENXS card requires a second input file. This line,
`tropt genxs inxcp200al nreact on nescat off`
specifies the use of GENXS and names the GENXS input file as `inxcp200al`. The file `inxcp200al` appears

below:

MCNP6 test: p, d, t, LF spectra from 200 MeV p + Al27 by CEM03.03
1 1 1 /
Cross Section Edit
72 -11 15 /
5. 10. 15. 20. 25. 30. 35. 40. 45. 50. 55. 60. 65. 70. 75. 80.
85. 90. 95. 100. 120. /
155. 145. 115. 105. 95. 85. 55. 45. 25. 15. 0. /
1 5 21 22 23 24 2006 3006 3007 3008 3009 4007 4009 4010 5010 /

See Ref. [5] for a full explanation of the GENXS input file. Note that the last line,
1 5 21 22 23 24 2006 3006 3007 3008 3009 4007 4009 4010 5010 /
contains the particle types to be tallied and output. Numbers $1-24$ refer to the MCNP6 particle types, as used in the previous GENXS version. With this expansion, heavy ions may now be tallied, according to their ZAID $(Z*1000+A)$. Therefore, numbers >1000 refer to the ZAID of a particular heavy ion. As an example, this GENXS input instructs MCNP6 to tally
1 5 21 22 23 24 2006 3006 3007 3008 3009 4007 4009 4010 5010
n p d t ^{3}He ^{4}He ^{6}He ^{6}Li ^{7}Li ^{8}Li ^{9}Li ^{7}Be ^{9}Be ^{10}Be ^{10}B.

Fig. 1 displays an excerpt of the double differential cross section output for ^{6}Li (ZAID 3006). Note that instead of showing "mu max" for the emission direction (as was done in the old version of GENXS), GENXS now outputs the angles in "degrees+/-spread". We believe this will be easier and more intuitive for users, and help avoid user error and misinterpretation. Angle-integrated spectra and energy-integrated spectra are also calculated, as well as the total angle- and energy-integrated production cross section.

The MCTAL tallies have also been updated so that angle-integrated cross section spectra of specified heavy ions may be viewed from within mcplot, similar to how specified nucleons and light fragments were viewed in the previous version of GENXS (see Fig. 2).

3. VALIDATION AND VERIFICATION

Fig. 3 shows plots of angle-integrated fragment spectra from MCNP6 compared to results by CEM03.03, for the reaction 200 MeV p + ^{27}Al. The results between MCNP6 and CEM03.03 are consistent. Furthermore, tests of the double differential cross sections also proved consistent. Lastly, other "test" reactions studied revealed the expected consistency between MCNP6 and CEM03.03.

We additionally tested this GENXS heavy-ion expansion with several different event generators (CEM03.03, Bertini+Dresner+RAL, INCL+ABLA, and LAQGSM03.03). Results of this test appear in Fig. 4. Results are as we expect.

3006 production cross section

E(MeV)	167.5deg+/-12.5	150.0deg+/- 5.0	130.0deg+/-15.0	110.0deg+/- 5.0	100.0deg+/- 5.0	90.0deg+/- 5.0	70.0deg+/-15.0
5.000000E+00	0.000E+00 0.000	0.000E+00 0.000	0.000E+00 0.000	0.000E+00 0.000	0.000E+00 0.000	0.000E+00 0.000	0.000E+00 0.000
1.000000E+01	8.301E-06 0.040	9.325E-06 0.039	1.165E-05 0.016	1.442E-05 0.023	1.529E-05 0.022	1.614E-05 0.021	1.803E-05 0.012
1.500000E+01	2.598E-06 0.072	2.822E-06 0.071	3.920E-06 0.028	6.006E-06 0.036	7.040E-06 0.032	8.988E-06 0.028	1.277E-05 0.014
2.000000E+01	6.929E-07 0.139	6.303E-07 0.151	1.011E-06 0.056	1.791E-06 0.065	2.538E-06 0.054	3.180E-06 0.047	5.867E-06 0.021
2.500000E+01	1.999E-07 0.258	1.146E-07 0.354	2.865E-07 0.105	5.259E-07 0.120	6.763E-07 0.104	1.110E-06 0.080	2.287E-06 0.034
3.000000E+01	9.327E-08 0.378	2.865E-08 0.707	1.039E-07 0.174	1.601E-07 0.218	3.200E-07 0.151	3.724E-07 0.139	7.161E-07 0.060
3.500000E+01	0.000E+00 0.000	1.432E-08 1.000	3.463E-08 0.302	3.049E-08 0.500	6.545E-08 0.333	1.003E-07 0.267	2.490E-07 0.102
4.000000E+01	1.332E-08 1.000	0.000E+00 0.000	9.445E-09 0.577	7.622E-09 1.000	1.454E-08 0.707	2.865E-08 0.500	6.673E-08 0.196
4.500000E+01	0.000E+00 0.000	0.000E+00 0.000	0.000E+00 0.000	0.000E+00 0.000	0.000E+00 0.000	7.162E-09 1.000	2.823E-08 0.302
5.000000E+01	0.000E+00 0.000	0.000E+00 0.000	6.297E-09 0.707	0.000E+00 0.000	0.000E+00 0.000	7.162E-09 1.000	1.283E-08 0.447
5.500000E+01	0.000E+00 0.000	0.000E+00 0.000	0.000E+00 0.000	0.000E+00 0.000	0.000E+00 0.000	0.000E+00 0.000	2.567E-09 1.000
6.000000E+01	0.000E+00 0.000	0.000E+00 0.000	0.000E+00 0.000	0.000E+00 0.000	0.000E+00 0.000	0.000E+00 0.000	2.567E-09 1.000
6.500000E+01	0.000E+00 0.000	0.000E+00 0.000	0.000E+00 0.000	0.000E+00 0.000	0.000E+00 0.000	0.000E+00 0.000	2.567E-09 1.000

E(MeV)	50.0deg+/- 5.0	35.0deg+/-10.0	20.0deg+/- 5.0	7.5deg+/- 7.5
5.000000E+00	0.000E+00 0.000	0.000E+00 0.000	0.000E+00 0.000	0.000E+00 0.000
1.000000E+01	1.901E-05 0.022	1.826E-05 0.019	1.853E-05 0.034	1.825E-05 0.045
1.500000E+01	1.709E-05 0.023	1.932E-05 0.018	2.134E-05 0.031	2.213E-05 0.041
2.000000E+01	8.508E-06 0.033	1.070E-05 0.024	1.315E-05 0.040	1.392E-05 0.051
2.500000E+01	3.852E-06 0.049	4.644E-06 0.037	6.638E-06 0.056	6.778E-06 0.074
3.000000E+01	1.683E-06 0.075	2.125E-06 0.054	2.680E-06 0.088	2.528E-06 0.120
3.500000E+01	4.862E-07 0.139	8.711E-07 0.085	1.026E-06 0.143	1.429E-06 0.160
4.000000E+01	2.618E-07 0.189	2.632E-07 0.154	5.863E-07 0.189	5.862E-07 0.250
4.500000E+01	6.544E-08 0.378	1.128E-07 0.236	6.282E-08 0.577	2.198E-07 0.408
5.000000E+01	2.805E-08 0.577	3.134E-08 0.447	6.282E-08 0.577	1.099E-07 0.577
5.500000E+01	0.000E+00 0.000	2.507E-08 0.500	0.000E+00 0.000	0.000E+00 0.000
6.000000E+01	0.000E+00 0.000	0.000E+00 0.000	0.000E+00 0.000	0.000E+00 0.000
6.500000E+01	0.000E+00 0.000	6.267E-09 1.000	0.000E+00 0.000	3.664E-08 1.000

E(MeV)	angle integrated	mu max	deg min	energy integrated
5.000000E+00	0.000E+00 0.000	-0.906307787037	155.0000000	5.949E-05 0.033
1.000000E+01	1.928E-04 0.006	-0.819152044289	145.0000000	6.467E-05 0.033
1.500000E+01	1.267E-04 0.008	-0.422618261741	115.0000000	8.510E-05 0.014
2.000000E+01	5.770E-05 0.012	-0.258819045103	105.0000000	1.147E-04 0.018
2.500000E+01	2.335E-05 0.018	-0.087155742748	95.0000000	1.297E-04 0.017
3.000000E+01	9.052E-06 0.029	0.087155742748	85.0000000	1.496E-04 0.015
3.500000E+01	3.255E-06 0.049	0.573576436351	55.0000000	2.002E-04 0.008
4.000000E+01	1.184E-06 0.081	0.707106781187	45.0000000	2.549E-04 0.014
4.500000E+01	3.608E-07 0.147	0.906307787037	25.0000000	2.818E-04 0.011
5.000000E+01	1.726E-07 0.213	0.965925826289	15.0000000	3.204E-04 0.018
5.500000E+01	3.922E-08 0.447	1.000000000000	0.0000000	3.299E-04 0.024
6.000000E+01	7.844E-09 1.000			
6.500000E+01	2.353E-08 0.577			

total 3006 production cross section = 2.073E-03 0.0045 yield = 5.28630E-03

Figure 1. Double differential cross section output from MCNP6 using GENXS for the reaction 200 MeV p + ^{27}Al $\rightarrow$ ^{6}Li, with angle- and/or energy-integrated cross sections also calculated.

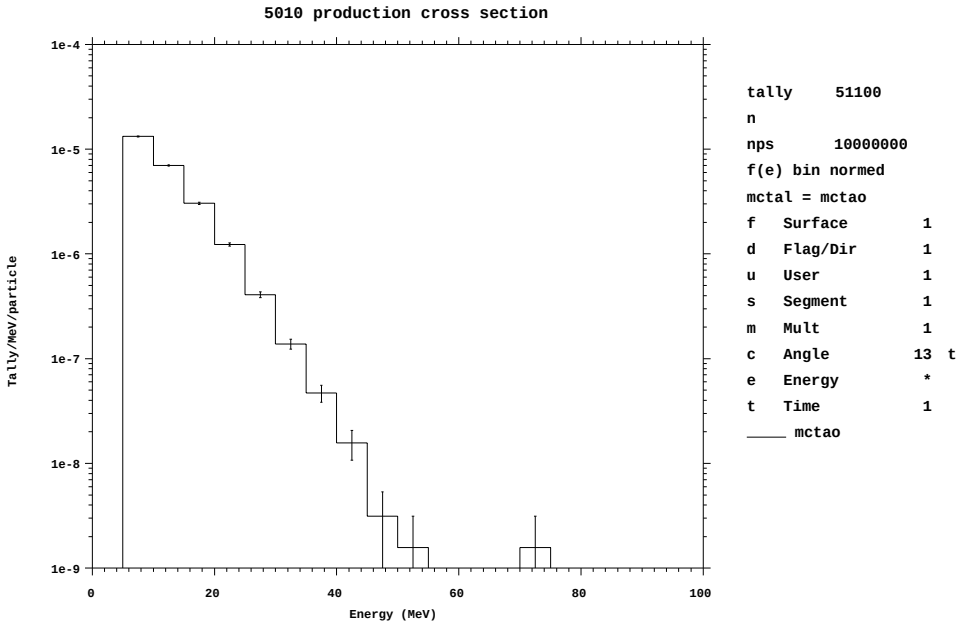

Figure 2. Example of MCTAL production cross section plot for the production of ZAID 5010 (^{10}B).

Furthermore, we tested MCNP6 with the GENXS heavy-ion expansion on a nucleus-induced reaction using the LAQGSM03.03 event generator. Results of this simulation compared with experimental data are seen in Fig. 5. Similar results were found in Example 6.5 of the MPI Testing Primer (LA-UR-13-26944).

We also tested our GENXS expansion running MPI, as well as with the 1400+ test suite. We conclude that this expansion works as expected across several different event generators and for both nucleon- and nucleus-induced reactions.

4. HEAVY CLUSTER PRODUCTION UPGRADES IN MCNP6

The expanded GENXS model allows us to test several new improvements in MCNP6 yielding more accurate heavy cluster production. These improvements come from heavy cluster upgrades made in CEM; we call this upgraded version CEM03.03F.

CEM03.03F was implemented into a working version of MCNP6, which we refer to as MCNP6-F. Two of the upgrades are always implemented: the upgraded NASA-Kalbach inverse cross sections in the

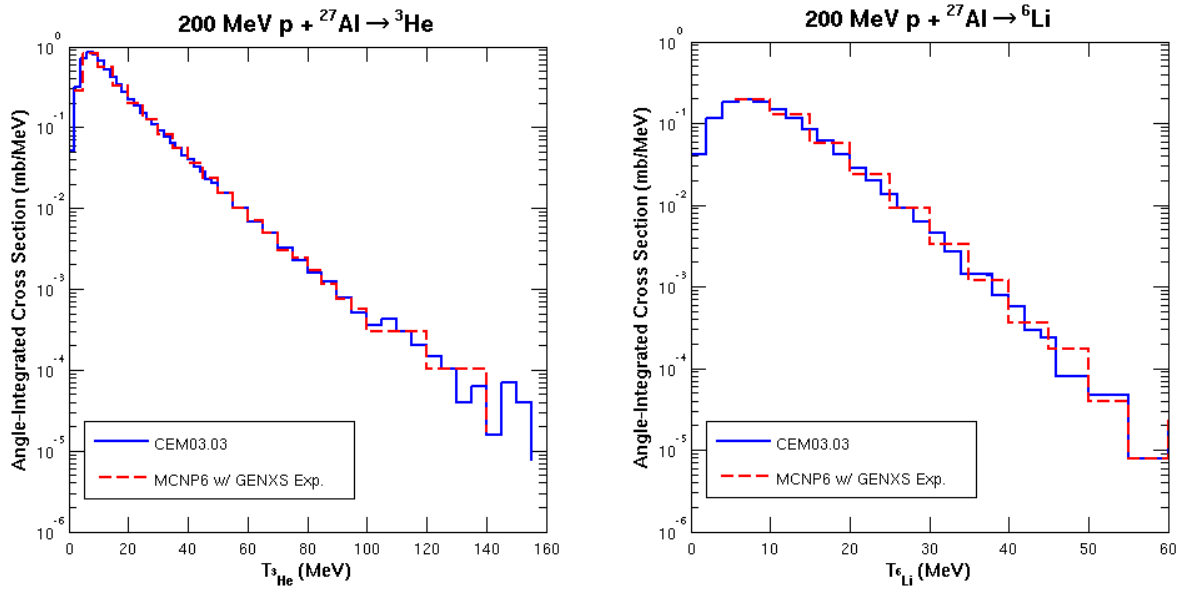

Figure 3. Comparison of emitted ^{3}He and ^{6}Li angle-integrated fragment spectra for the reaction 200 MeV p + ^{27}Al, calculated by MCNP6 (red dashed lines) and CEM03.03 (blue solid lines).

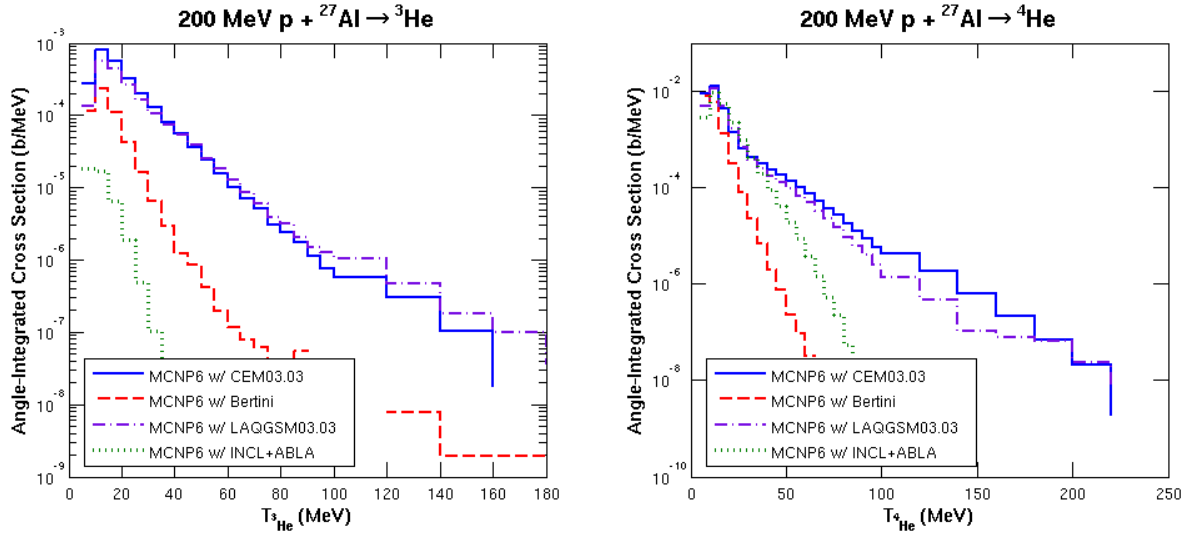

Figure 4. Comparison of emitted ^{3}He and ^{4}He angle-integrated fragment spectra for the reaction 200 MeV p + ^{27}Al, calculated by MCNP6 with CEM03.03 (blue solid lines), with Bertini (red dashed lines), with LAQGSM03.03 (purple dash-dotted lines), and with INCL-ABLA (green dotted lines), all run with the GENXS expansion for heavy ions discussed in this paper.

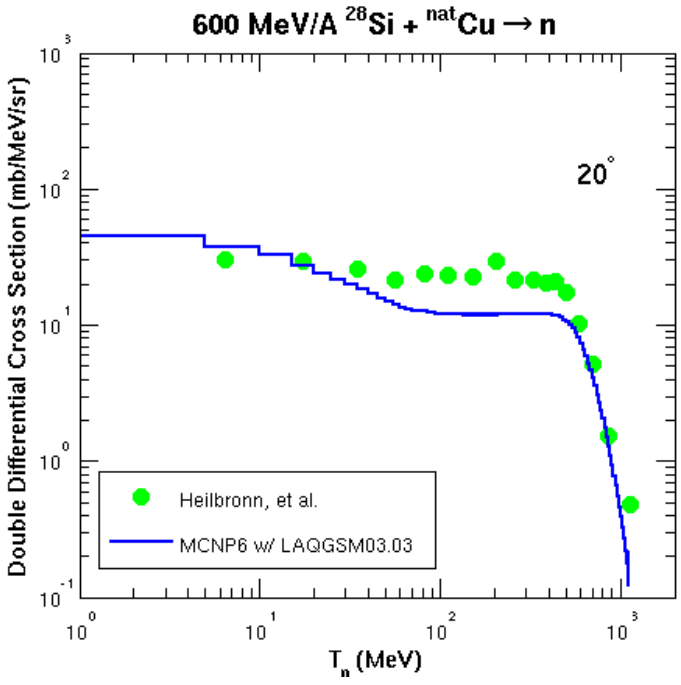

Figure 5. Comparison of emitted neutron double differential spectra for the reaction 600 MeV/A ^{28}Si + ^{nat}Cu, at an emission angle of 20°, calculated by MCNP6 with LAQGSM03.03 with this GENXS heavy-ion expansion (blue solid line), compared to results by Heilbronn, et al. [7] (green points).

preequilibruim stage, and the new energy-dependent γ_j model. The other two upgrades (extension of preequilibrium emission to ^{28}Mg, and the extension of the coalescence model to ^{7}Be), both of which increase computation time, may be turned off if desired. For details, see Ref. [6]. A variable, called npreqtyp, was created to specify the number of preequilibrium particles considered for emission. It is now the twelfth option on the LCA card of the MCNP6 input file. Its maximum (and default) value is 66, similar to the nevtype variable used for the evaporation stage. See Table I for a list of the 66 particles considered in the preequilibrium stage. In the old model, 6 preequilibrium particles were considered, and therefore a value of npreqtyp=6 turns off both the preequilibrium and coalescence extensions. The extended coalescence model is implemented for values of npreqtyp>6. MCNP6-F also includes the GENXS extension.

Basic testing and verification of MCNP6-F has been completed with the results being presented below. In addition, MPI testing has been completed. Upon further testing, we anticipate these heavy-ion upgrades and the GENXS extension will be included in the next release of MCNP6.

Double differential cross section spectra for several reactions are plotted in Figs. 6 and 7, comparing experimental data with results from CEM03.03F (blue solid lines), MCNP6-F with npreqtyp=66 (red dashed lines), and MCNP6 with the GENXS extension only (purple dash-dotted lines). MCNP6 with the GENXS extension only does not contain any of the four light-fragment upgrades contained in CEM03.03F (but includes the GENXS extension so that we can output double differential cross sections

Table I. The emitted fragments included in the modified preequilibrium.

Z_j	Ejectiles						
0	n						
1	p	d	t				
2	^{3}He	^{4}He	^{6}He	^{8}He			
3	^{6}Li	^{7}Li	^{8}Li	^{9}Li			
4	^{7}Be	^{9}Be	^{10}Be	^{11}Be	^{12}Be		
5	^{8}B	^{10}B	^{11}B	^{12}B	^{13}B		
6	^{10}C	^{11}C	^{12}C	^{13}C	^{14}C	^{15}C	^{16}C
7	^{12}N	^{13}N	^{14}N	^{15}N	^{16}N	^{17}N	
8	^{14}O	^{15}O	^{16}O	^{17}O	^{18}O	^{19}O	^{20}O
9	^{17}F	^{18}F	^{19}F	^{20}F	^{21}F		
10	^{18}Ne	^{19}Ne	^{20}Ne	^{21}Ne	^{22}Ne	^{23}Ne	^{24}Ne
11	^{21}Na	^{22}Na	^{23}Na	^{24}Na	^{25}Na		
12	^{22}Mg	^{23}Mg	^{24}Mg	^{25}Mg	^{26}Mg	^{27}Mg	^{28}Mg

for light fragments). The new MCNP6-F with the light-fragment upgrades, in general, gives improved results compared to the unmodified MCNP6, most especially for heavy-cluster spectra.

Fig. 6 displays the results for 200 MeV p + ^{197}Au $\rightarrow$ ^{6}Li at 45°, compared to experimental data by Machner, et al. [8]. This figure also contains spectra from MCNP6-F with `npreqtyp=6`; these results should be similar to MCNP6 with the GENXS extension only, as the only difference between the two is that MCNP6-F contains the improved inverse cross sections and the γ_j Model. This figure shows not only dramatically improved heavy-cluster production by MCNP6-F at high energies, but also improved production at relatively low energies around the preequilibrium peak. We believe this is due to the heavy target (gold) and therefore an increased ability to produce these low-energy heavy clusters from both the extended coalescence model and the extended preequilibrium model.

Fig. 7 demonstrates the results for 2500 MeV p + ^{nat}Ni $\rightarrow$ t, ^{7}Li at 100°, compared to experimental data measured by Budzanowski, et al. [9]. The triton spectra illustrate that MCNP6-F achieves increased production of heavy clusters without destroying the established spectra of nucleons and light fragments with $A < 5$.

5. CONCLUSION

The GENXS option in MCNP6 can be used to tally fragment production cross sections for applications at high-energies (> 150 MeV): including space research, medical physics, and accelerator applications. Previously, production cross sections were only available for fragments up to ^{4}He. We have expanded GENXS to tally and output production cross sections for any heavy ion (with valid ZAID). This expansion has been validated and verified and we expect it to be useful to scientists within these applications.

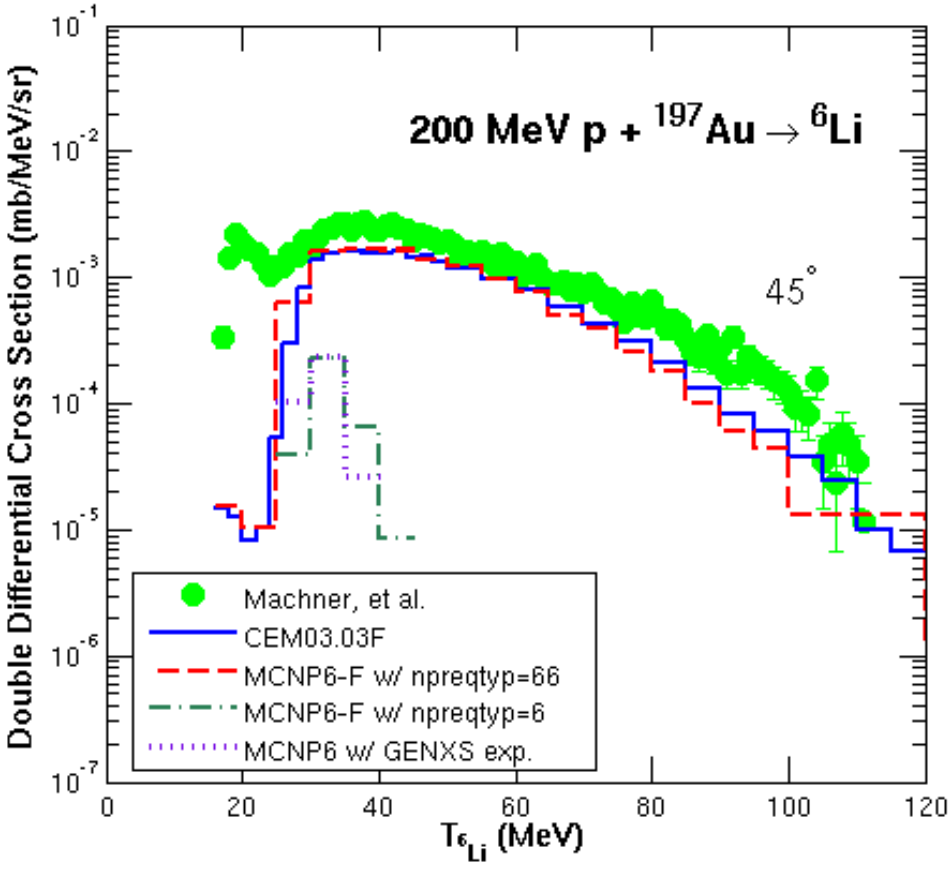

Figure 6. Comparison of experimental data for 200 MeV p + ^{197}Au → ^{6}Li at 45°, measured by Machner, et al. [8] (green circles) to calculations from CEM03.03F (blue solid lines), MCNP6-F with npreqtyp=66 (red dashed lines), MCNP6-F with npreqtyp=6 (green dash-dotted lines), and MCNP6 with the GENXS extension only (purple dotted lines).

ACKNOWLEDGMENTS

This study was carried out under the auspices of the National Nuclear Security Administration of the U.S. Department of Energy at Los Alamos National Laboratory under Contract No. DE-AC52-06NA25396.

REFERENCES

[1] T. Goorley, M. James, T. Booth, F. Brown, J. Bull, L. Cox, J. Durkee, J. Elson, M. Fensin, R. Forster, J. Hendricks, G. Hughes, R. Johns, B. Kiedrowski, R. Martz, S. Mashnik, G. McKinney,

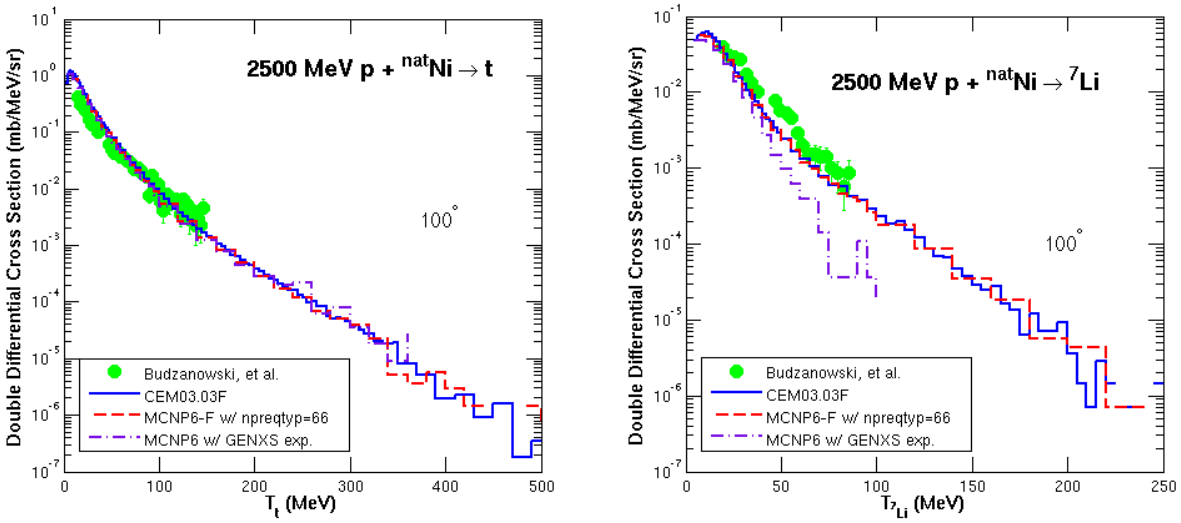

Figure 7. Comparison of experimental data for 2500 MeV p + ^{nat}Ni $\rightarrow$ t,^{7}Li at 100°, measured by Budzanowski, et al. [9] (green circles) to calculated results from CEM03.03F (blue solid lines), MCNP6-F with npreqtyp=66 (red dashed lines), and MCNP6 with the GENXS extension only (purple dash-dotted lines).

D. Pelowitz, R. Prael, J. Sweezy, L. Waters, T. Wilcox, and T. Zukaitis, "Initial MCNP6 Release Overview, MCNP6 version 0.1," *Nuclear Technology* **180**: p. 298 (2012).

[2] K. Gudima, S. Mashnik, and V. Toneev, "Cascade-Exciton Model of Nuclear Reactions," *Nuclear Physics* **A401**: pp. 329–361 (1983).

[3] S. Mashnik, K. Gudima, R. Prael, A. Sierk, M. Baznat, and N. Mokhov, "CEM03.03 and LAQGSM03.03 Event Generators for the MCNP6, MCNPX, and MARS15 Transport Codes," Joint ICTP-IAEA Advanced Workshop on Model Codes for Spallation Reactions. Trieste, Italy, February 2008, *LANL Report*, LA-UR-08-2931, (2008); arXiv:0805.0751.

[4] K. Gudima, S. Mashnik, and A. Sierk, "User Manual for the Code LAQGSM," *LANL Report*, LA-UR-01-6804 (2001); http://lib-www.lanl.gov/lapubs/00818645.pdf.

[5] R. Prael, "Tally Edits for the MCNP6 GENXS Option," *LANL Report*, LA-UR-11-02146, (2011).

[6] L. Kerby, S. Mashnik, K. Gudima, A. Sierk, J. Bull, and M. James", "Production of Energetic Heavy Clusters in CEM and MCNP6," *LANL Report*, LA-UR-15-29524 (2015).

[7] L. Heilbronn, C. Zeitlin, Y. Iwata, T. Murakami, H. Iwase, T. Nakamura, T. Nunomiya, H. Sato, H. Yashima, R. M. Ronningen, and K. Ieki, "Secondary Neutron-Production Cross Sections from Heavy-Ion Interactions Between 230 and 600 MeV/Nucleon," *Nuclear Science and Engineering*, **157**: p. 142 (2007).

[8] H. Machner, D. Aschman, K. Baruth-Ram, J. Carter, A. Cowley, F. Goldenbaum, B. Nangu, J. Pilcher, E. Sideras-Haddad, J. Sellschop, F. Smit, B. Spoelstra, and D. Steyn, "Isotopic production cross sections in proton-nucleus collisions at 200 MeV," *Physical Review C*, **73**: p. 044606 (2006).

[9] A. Budzanowski, M. Fidelus, D. Filges, F. Goldenbaum, H. Hodde, L. Jarczyk, B. Kamys, M. Kistryn, St. Kistryn, St. Kliczewski, A. Kowalczyk, E. Kozik, P. Kulessa, H. Machner, A. Magiera, B. Piskor-Ignatowicz, K. Pysz, Z. Rudy, R. Siudak, and M. Wojciechowski, "Comparison of nonequilibrium processes in p+Ni and p+Au collisions at GeV energies," *Physical Review C*, **82**: p. 034605 (2010).